

## A parallel integration method for solar system dynamics

Prasenjit Saha  
Mount Stromlo and Siding Spring Observatories,  
Australian National University,  
Canberra ACT 0200, Australia  
saha@mso.anu.edu.au

Joachim Stadel  
Astronomy Department FM-20,  
University of Washington, Seattle, WA 98195-1580  
stadel@astro.washington.edu

Scott Tremaine  
Canadian Institute for Theoretical Astrophysics,  
McLennan Labs, University of Toronto,  
60 St. George St., Toronto M5S 3H8, Canada  
tremaine@cita.utoronto.ca

**Abstract:** We describe how long-term solar system orbit integration could be implemented on a parallel computer. The interesting feature of our algorithm is that each processor is assigned not to a planet or a pair of planets but to a time-interval. Thus, the 1st week, 2nd week, ..., 1000th week of an orbit are computed concurrently. The problem of matching the input to the  $(n + 1)$ -st processor with the output of the  $n$ -th processor can be solved efficiently by an iterative procedure. Our work is related to the so-called waveform relaxation methods in the computational mathematics literature, but is specialized to the Hamiltonian and nearly integrable nature of solar system orbits. Simulations on serial machines suggest that, for the reasonable accuracy requirement of  $1''$  per century, our preliminary parallel algorithm running on a 1000-processor machine would be about 50 times faster than the fastest available serial algorithm, and we have suggestions for further improvements in speed.

## 1. INTRODUCTION

Planetary orbits have now been studied over times of  $10^8$ – $10^{10}$  yr using various techniques, and exploring progressively longer time scales always seems to reveal interesting new phenomena. Laskar (1989, 1990, 1994) used a semi-analytic secular perturbation theory to follow planetary orbits for up to 10 Gyr, and found weak chaos in the orbits of the inner planets, which led for example to significant evolution in Mercury’s orbit over the lifetime of the solar system. Sussman & Wisdom (1992) directly integrated the orbits of the nine planets for 100 Myr, verifying Laskar’s discovery that the orbits of the inner planets are chaotic, and also finding weak chaos in the orbits of the outer planets which did not appear in Laskar’s secular theory. Laskar & Robutel (1993) and Touma & Wisdom (1993) by different methods found that Mars’s obliquity is chaotic, whereas the Earth’s is apparently stabilized by the Moon. Naturally, long integrations are not ephemerides but probes of qualitative and statistical properties of the orbits. We remark that it is possible to extract information about dependence on initial conditions from Fourier analysis of a single integration (Laskar 1993).

Since the longest direct orbit integrations are still much shorter than the age of the solar system, there is motivation to invent better numerical integration algorithms. The best long-term accuracy is achieved by methods that exploit (a) the Hamiltonian, and (b) the nearly Keplerian properties of the equations. Such methods were introduced by Wisdom & Holman (1991; hereafter WH91) and independently by Kinoshita, Yoshida & Nakai (1991), with subsequent improvements by various authors; for brevity, we will call them ‘generalized leapfrog’ in this paper, because of their formal resemblance to leapfrog. An  $n$ -th order generalized leapfrog integrator can have global error of  $O(\epsilon^2 \tau^n T)$ , where  $\epsilon \lesssim 10^{-3}$  is the relative scale of planetary perturbations,  $\tau$  is the timestep, and  $T$  the total length of an integration. The  $\epsilon^2$  factor and the linear dependence on  $T$  (rather than quadratic, as for general purpose integrators) make low-order schemes worthwhile. The state of the art demands an accuracy of  $\sim 10^{-9}$  in the frequencies (or  $\sim 1''$  per century for Mercury), which is achievable by second-order generalized leapfrog schemes with  $\tau \simeq 1$  week—see Wisdom, Holman & Touma (1994) or Saha & Tremaine (1994; hereafter ST94). But a 5 Gyr integration remains prohibitively expensive at current floating-point speeds.

This situation prompts one to think about parallel integration methods, and in this paper we develop a parallel integrator. We adopt a very different sort of parallelism from galactic or cosmological parallel codes; instead of distributing the force calculation among different processors, we distribute different time slices among different processors. Solar system dynamics invites such ‘timelike’ rather than the usual ‘spacelike’ parallelism because orbits evolve very slowly compared to orbital times, whereas the number of forces that could be distributed between processors is relatively small. The new algorithm is very similar to second-order generalized leapfrog in accuracy, and is better at controlling roundoff error; but it is arithmetically more cumbersome, so—at least in the present version of a parallel integrator—the speed gain possible is smaller than the number of processors.

## 2. A PARALLEL ALGORITHM

Consider some system of ordinary differential equations  $\dot{z} = f(z)$ , or equivalently, a set of quadratures:

$$z(t) = z(0) + \int_0^t f(z(t')) dt'. \quad (1)$$

We can approximate the quadratures by sums; discretizing time with timestep  $\tau$  and writing  $z_n$  to mean  $z(n\tau)$ , we can write, for example:

$$z_n = z_0 + \tau \sum_{m=0}^{n-1} f\left(\frac{1}{2}(z_m + z_{m+1})\right); \quad n = 1..N. \quad (2)$$

This can now be regarded as a set of nonlinear equations in many variables ( $N$  times the dimensionality of  $z$ ), which can be solved by some iterative process. In an  $N$ -processor computer, the right side of equation (2) can be evaluated in parallel, with each processor computing one term and  $O(\log N)$  sums. If the number of iterations is much less than the number of processors, then parallelism will yield a speed gain.

Solving the huge set of equations (2) in  $\ll N$  iterations may seem a hopeless task. But in fact it can often be accomplished (provided the original differential equations are very smooth and there is a good starting guess for the  $z_n$ ) by Newton-Raphson or variants of it not requiring derivatives (see e.g., Ortega & Rheinbolt 1970). The general idea is known as *waveform relaxation*; we suggest Bellen & Zennaro (1989) as an introduction to the literature in this area. In this paper, however, we will proceed from first principles, because for nearly integrable Hamiltonian systems the solution becomes quite simple.

For a Hamiltonian system with canonical variables  $z \equiv (p, q)$  the particular quadrature formula in equation (2) amounts to integrating the differential equations with the ‘implicit midpoint’ integrator

$$\begin{aligned} p_1 &= p_0 - \tau \frac{\partial}{\partial q} H\left(\frac{1}{2}(z_0 + z_1)\right), \\ q_1 &= q_0 + \tau \frac{\partial}{\partial p} H\left(\frac{1}{2}(z_0 + z_1)\right), \end{aligned} \quad (3)$$

with timestep  $\tau$  (which can be kept fixed when integrating planetary orbits). This is a second order symplectic integrator, which is to say that the transformation  $z_0 \rightarrow z_1$  differs from the true time evolution by  $O(\tau^3)$  but is exactly canonical. It is one of a class of symplectic integrators derived by Feng (1986). In the Appendix we derive a somewhat stronger statement: the integrator exactly follows the dynamics of a ‘surrogate’ Hamiltonian

$$\tilde{H} = H + H_{\text{err}}, \quad (4)$$

which differs from the exact Hamiltonian  $H$  by an error Hamiltonian  $H_{\text{err}}$  which is  $O(\tau^2)$  and non-autonomous ( $H_{\text{err}}$  is periodic in time with period  $\tau$ ). In any case, the symplectic property guarantees that spurious dissipation will not occur.

Consider now an  $H$  that is close to some integrable Hamiltonian, with  $p, q$  being action-angle variables for the latter, thus:

$$H = H^{(0)}(p) + \epsilon H^{(1)}(p, q, t). \quad (5)$$

The formula (2) for such a system becomes

$$\begin{aligned} p_n &= p_0 - \tau \sum_{m=0}^{n-1} \epsilon \frac{\partial}{\partial q} H^{(1)} \left( \frac{1}{2}(z_m + z_{m+1}) \right), \\ q_n &= q_0 + \tau \sum_{m=0}^{n-1} \left[ \frac{\partial}{\partial p} H^{(0)} \left( \frac{1}{2}(p_m + p_{m+1}) \right) + \epsilon \frac{\partial}{\partial p} H^{(1)} \left( \frac{1}{2}(z_m + z_{m+1}) \right) \right]. \end{aligned} \quad (6)$$

The error Hamiltonian is  $O(\epsilon\tau^2)$  (see Appendix). The error has the same order as in second-order generalized leapfrog, suggesting that the performance will be similar. Generalized leapfrog is preferable for serial integrations because it is explicit, but as part of an iterative parallel scheme explicit methods offer no advantage, and implicit midpoint leads to a simpler formulation.

We now need to solve the equations (6) for the  $p_n, q_n$ . Let us abbreviate the equations as

$$\begin{aligned} p_n - p_0 - u(P_n, Q_n) &= 0, \\ q_n - q_0 - V(P_n) - v(P_n, Q_n) &= 0, \end{aligned} \quad (7)$$

where  $u$  and  $v$  are  $O(\epsilon)$  smaller than  $V$ , and  $P_n, Q_n$  are the vectors  $(p_0 \dots p_n), (q_0 \dots q_n)$ . Suppose that  $P_n, Q_n$  are currently at some good guess values for the exact solutions  $P'_n, Q'_n$ . We start out as if to derive a Newton-Raphson iteration, and expand (7) to leading order in  $z_n - z'_n$ :

$$\begin{aligned} p_n - p_0 - u(P_n, Q_n) &\simeq [p'_n - p_0 - u(P'_n, Q'_n)] + p_n - p'_n \\ &\quad - \langle \text{terms involving derivatives of } u \rangle \\ q_n - q_0 - V(P_n) - v(P_n, Q_n) &\simeq [q'_n - q_0 - V(P'_n) - v(P'_n, Q'_n)] + q_n - q'_n \\ &\quad - \sum_{m=1}^n (p_m - p'_m) \partial / \partial p_m V(P_n) - \langle \text{terms involving derivatives of } v \rangle \end{aligned} \quad (8)$$

The terms in square brackets are zero since  $z'$  solves (7). We then substitute  $V(P_n) - V(P'_n)$  for  $\sum_{m=1}^n (p_m - p'_m) (\partial / \partial p_m) V(P_n)$  and neglect derivatives of  $u$  and  $v$  (thus departing from Newton-Raphson and sacrificing quadratic convergence), to obtain

$$\begin{aligned} p'_n &\leftarrow p_0 + u(P_n, Q_n), \\ q'_n &\leftarrow q_0 + V(p'_n) + v(P_n, Q_n), \end{aligned} \quad (9)$$

Once in the neighborhood of the correct solution, the simple iteration (9) will give linear convergence by a factor  $O(\epsilon)$  per iteration. The obvious starting guess to use is the solution to the unperturbed equations, which is trivial since  $p, q$  are action-angles. Better guesses are possible, such as the mean semi-major axes and the eccentricities and inclinations given by secular perturbation theory; however, our tests with toy problems suggest that these will not lead to dramatic reductions in the number of iterations required for convergence. Note that making  $N$  excessively large will not introduce the danger of divergence of iterations, because the sequence of approximants to  $z_n$  does not influence the approximants at any  $z_{m < n}$ . Provided the iterative process converges for the serial formula (3), the worst that can happen in the parallel case is that the convergence becomes proportional to  $N$ .

## 3. AN SIMPLE EXAMPLE

It is helpful to apply the iterative procedure of the previous section as applied to a simple example. We consider the pendulum Hamiltonian

$$H = \frac{1}{2}p^2 - \epsilon \cos q. \quad (10)$$

For this case, because integrals of the type (1) can be done exactly, we will leave them as integrals rather than replacing them by sums. We also make one change of notation for this section:  $p_k$  and  $q_k$  will refer to the  $k$ -th approximation to  $p(t)$  and  $q(t)$ , and not to values on a grid.

With these changes the iterative scheme (9) becomes

$$\begin{aligned} p_0(t) &= p(0), \\ q_0(t) &= q(0) + p(0)t, \\ p_{k+1}(t) &= p(0) - \epsilon \int_0^t \sin[q_k(t')] dt', \\ q_{k+1}(t) &= q(0) + \int_0^t p_{k+1}(t') dt'. \end{aligned} \quad (11)$$

We can derive expressions for the errors in the  $n$ -th approximation

$$\delta p_k(t) \equiv p_k(t) - p(t), \quad \delta q_k(t) \equiv q_k(t) - q(t), \quad (12)$$

by comparing the iterates (11) with the exact equations

$$\begin{aligned} p(t) &= p(0) - \epsilon \int_0^t \sin[q(t')] dt', \\ q(t) &= q(0) + \int_0^t p(t') dt'. \end{aligned} \quad (13)$$

Assuming  $|\delta q_k| \ll 1$  and hence  $\sin[q_k(t)] \simeq \sin[q(t)]$  for all  $k \geq 0$ , we get:

$$\begin{aligned} \delta p_0(t) &= \epsilon \int_0^t \sin[q_0(t')] dt', \\ \delta q_0(t) &= \int_0^t \delta p_0(t') dt', \\ \delta p_{k+1}(t) &= -\epsilon \int_0^t \cos[q_0(t')] \delta q_k(t') dt', \\ \delta q_{k+1}(t) &= \int_0^t \delta p_{k+1}(t') dt'. \end{aligned} \quad (14)$$

These equations can be solved analytically, although the expressions for  $\delta p_k(t)$  and  $\delta q_k(t)$  rapidly become quite complicated as  $k$  grows. For large values of  $\epsilon t$  we find that to leading order the even iterates satisfy

$$|\delta q_{2k}(t)| = \frac{|\cos q(0)|}{2^k (2k+1)!} \left( \frac{\epsilon t}{p(0)} \right)^{2k+1} + O(t^{2k-1}); \quad |\delta p_{2k}(t)| = \frac{(2k+1)}{t} |\delta q_{2k}(t)| + O(t^{2k-1}). \quad (15)$$

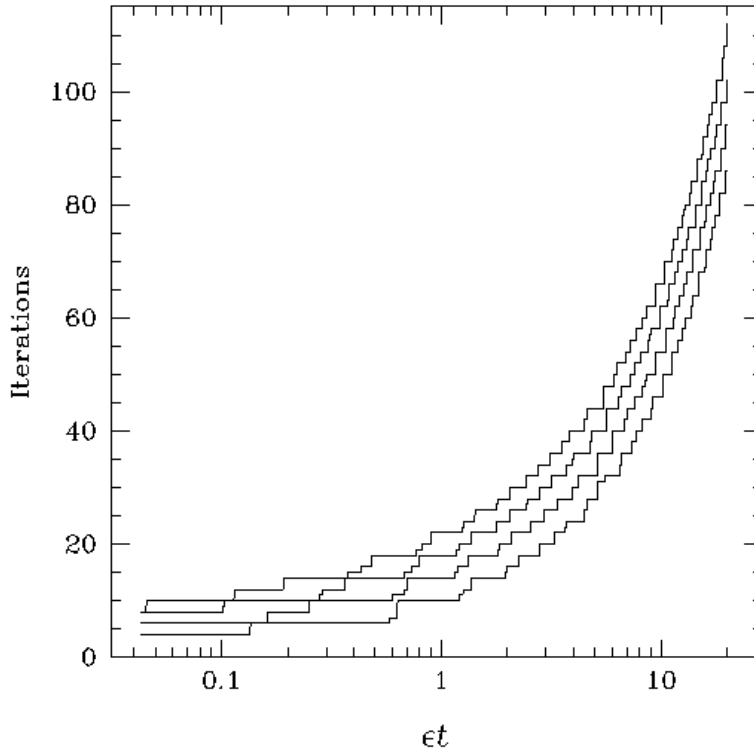


**Figure 1.** Diagnostics from a numerical solution for the pendulum Hamiltonian (10) with  $\epsilon = 0.01$ ,  $p(0) = 1, q(0) = 0$ , integrated using the algorithm of Section 2, with timestep  $\tau = 0.1$ . The four curves are the number of iterations required for convergence to  $10^{-4}$ ,  $10^{-6}$ ,  $10^{-8}$ , and  $10^{-10}$ . The corresponding plot for  $\tau = 0.01$  is almost identical.

Thus the iterative scheme will converge for all  $\epsilon t$ . For small  $\epsilon t$  the number of iterations required will be roughly  $n_{\text{it}} \propto -1/\ln(\epsilon t)$ . For  $\epsilon t \gg 1$ , we expect that if  $p(0) = 1$ , then  $n_{\text{it}} \propto \epsilon t$  iterations will be required for convergence.

We plot in Figure 1 the number of iterations taken by the scheme (9) to converge to various levels as a function of time. This case differs in detail from the one we have just analyzed, because it refers to a discretized situation as in Section 2; this means that the iterations are converging not to the true solution, but to a surrogate differing from the true solution by a timestep-dependent amount. Also, the approximation  $\sin[q_k(t)] \simeq \sin[q(t)]$  we made above is not always valid. Nevertheless, Figure 1 agrees with our qualitative prediction of number of iterations  $\propto \epsilon t$  for large  $\epsilon t$ ; quantitatively, the number of iterations is  $\approx 4\epsilon t$ .

## 4. SURROGATES, AND WARMUP

If a generalized leapfrog integrator is applied to a nearly integrable Hamiltonian, the output can be expressed formally as the time evolution under the surrogate Hamiltonian

$$\tilde{H} = H + \epsilon\tau^n \times \langle \text{power series in } \epsilon \text{ and } \tau^2 \rangle, \quad (16)$$

for an  $n$ -th order scheme. We say ‘formally’ because the series in equation (16) does not in general converge; nevertheless, analysis of this series is useful. In particular, the  $\epsilon\tau^n$  indicates long term errors of  $O(\epsilon\tau^n T)$ . It turns out that one can eliminate the effect of secular  $O(\epsilon)$  terms in  $\tilde{H}$  by applying a special small transformation to either the initial conditions or the output, thus reducing the errors to  $O(\epsilon^2\tau^n T)$ . Various transformations which accomplish this are given in Saha & Tremaine (1992), WHT94, and ST94. Probably the simplest comes from the latter paper, and consists of the following ‘warmup’ to the main integration.

$$\begin{aligned} &\langle \text{Integrate backward (or forward) for a large number of orbits with the timestep } \tau \\ &\quad \text{scaled down by } \lesssim \epsilon^{1/n} \text{ while linearly reducing the perturbation strength to zero} \rangle \\ &\langle \text{Integrate forward (or backward) to the starting point with the regular timesteps } \tau, \\ &\quad \text{while linearly reviving the perturbation strength to the correct value} \rangle \end{aligned} \quad (17)$$

In the Appendix, we show that errors in the implicit midpoint integrator also can be described by a surrogate Hamiltonian, which differs from  $H$  by an error Hamiltonian that is  $O(\epsilon\tau^2)$  if  $H$  is nearly integrable. Thus the above warmup procedure will reduce long-term errors from  $O(\epsilon\tau^2 T)$  to  $O(\epsilon^2\tau^2 T)$  whether we use generalized leapfrog or implicit midpoint. In fact, the results from the implicit midpoint method, both without and with warmup, are very similar to those from the corresponding generalized leapfrog method.

## 5. A SIMULATION WITH NINE PLANETS

To apply the new integration method to planetary orbits, we must:

- (i) reduce the Hamiltonian to the form  $H^{(0)} + \epsilon H^{(1)}$ , where now  $H^{(0)}$  is Keplerian and  $\epsilon$  represents the smallness of planetary perturbations;
- (ii) find action-angle variables  $p, q$  for  $H^{(0)}$ ;
- (iii) find expressions for  $(\partial H^{(1)}/\partial p)$  and  $(\partial H^{(1)}/\partial q)$ .

Item (i) is standard, though not trivial. Barycentric variables will not do because the Sun’s motion is not nearly Keplerian. The key (see WH91) is to take Mercury’s coordinates relative to the Sun, Venus’s relative to the barycenter of Sun-Mercury, and so on (the ordering of planets is immaterial). The time derivatives of such coordinates—called the Jacobi coordinates—turn out to be proportional to the conjugate momenta. The Sun’s motion drops out and is replaced by the ignorable motion of the solar system barycenter. The Hamiltonian has the desired form, with one Keplerian term for each planet plus perturbation terms of  $O(\epsilon)$ . Post-Newtonian effects from general relativity add a further complication; a procedure for handling these effects is described in ST94.

For item (ii), we transform the Jacobi variables for each planet to Poincaré elements  $\Lambda, \lambda, \xi_1, \xi_2, \eta_1, \eta_2$ . These relate to the more familiar Keplerian elements  $a, e, i, \Omega, \omega, M$  as follows:

$$\begin{aligned}
 \Lambda &= \sqrt{\mu a}, & \lambda &= \Omega + \omega + M, \\
 \xi_1 &= \left[ 2\Lambda(1 - \sqrt{1 - e^2}) \right]^{\frac{1}{2}} \cos(\Omega + \omega) \simeq \sqrt{\Lambda} e \cos(\Omega + \omega), \\
 \xi_2 &= - \left[ 2\Lambda(1 - \sqrt{1 - e^2}) \right]^{\frac{1}{2}} \sin(\Omega + \omega) \simeq -\sqrt{\Lambda} e \sin(\Omega + \omega), \\
 \eta_1 &= \left[ 2\Lambda\sqrt{1 - e^2}(1 - \cos i) \right]^{\frac{1}{2}} \cos \Omega \simeq \sqrt{\Lambda} i \cos \Omega, \\
 \eta_2 &= - \left[ 2\Lambda\sqrt{1 - e^2}(1 - \cos i) \right]^{\frac{1}{2}} \sin \Omega \simeq -\sqrt{\Lambda} i \sin \Omega.
 \end{aligned} \tag{18}$$

The first two are action-angles of  $H^{(0)}$ ; the other four are not action-angles but they are canonical, which is good enough since  $H^{(0)}$  involves only the  $\Lambda$  of each planet. Poincaré elements remain non-singular for zero  $e$  or  $i$ .

Item (iii) consists of transforming the accelerations to Poincaré variables. This is straightforward with the chain rule, but boring to program and expensive to compute. With nine planets, we found that transforming accelerations from cartesian Jacobi variables to Poincaré elements took more than four times as long as evaluating the accelerations in the first place.

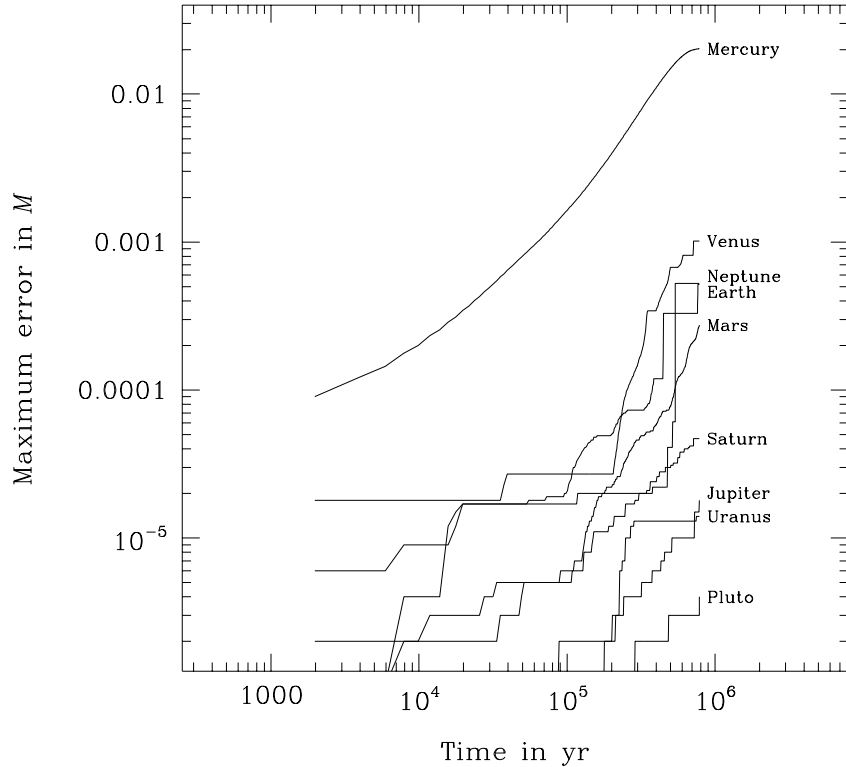


**Figure 2.** Maximum error in mean anomaly  $M$  up to time  $T$ , against  $T$ , with a timestep of  $7\frac{1}{32}$  days.

We have programmed the algorithm to simulate its operation on a parallel computer, and tested the results of a medium-length integration. We used a timestep of  $7\frac{1}{32}$  days and a warmup length of 5000 yr with timestep scaled down by 32. Our single actual processor was simulating 4096 concurrent ones. Figure 2 shows the estimated errors in our integration, gotten by comparing with a more accurate version of the integration by Quinn, Tremaine & Duncan (1991). It is quite similar to Figure 2 in ST94 which shows error estimates for generalized leapfrog with the same timestep.

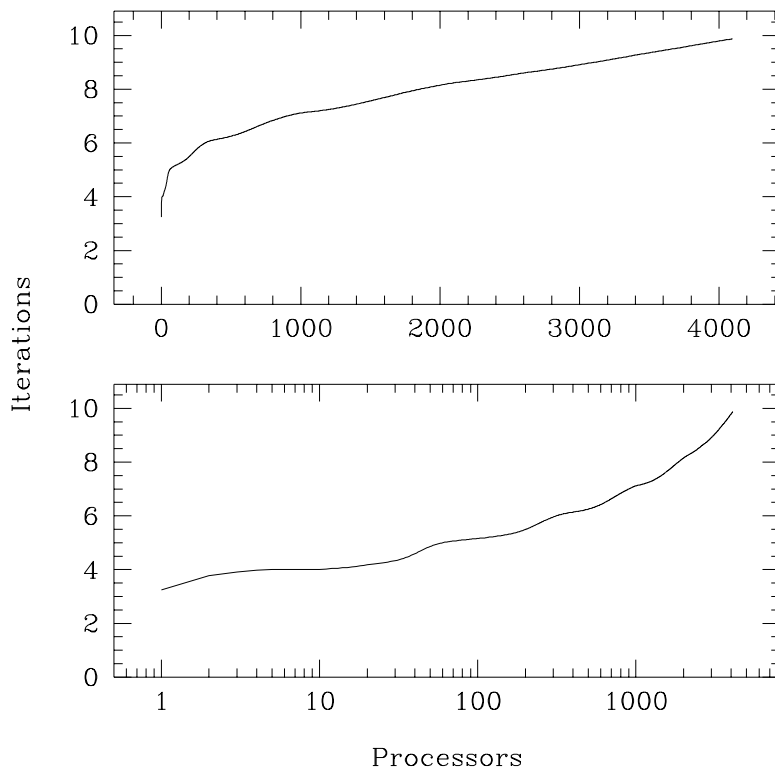


**Figure 3.** The average number of iterations required for convergence (to  $\simeq 50$  bits of precision) versus the number  $N$  of simulated processors. The two panels show the same data using linear and logarithmic scales for  $N$ .

In Figure 3 we show the average number of iterations  $n_{\text{it}}$  our algorithm needed to converge to  $\simeq 50$  bits of precision (relative error  $\simeq 10^{-15}$ ), over blocks of steps of different lengths  $N$  (in effect, different numbers of processors). The plots exhibit the linear dependence at large  $N$  predicted by the simple model of Section 3, and can be fitted by

$$n_{\text{it}} \simeq 6 + \left( \frac{N}{1000} \right) \quad \text{for } N > 500. \quad (19)$$

While the above results demonstrate that our algorithm works, our current implementation is probably far from optimal. In particular, our program does about 10 times as much arithmetic per iteration as generalized leapfrog with individual timesteps to complete an integration of the same length. The picture changes, though, when we consider the control of roundoff errors. We consider this and other prospects for improvement in the concluding section.

## 6. PROSPECTS

A serious obstacle to accurate long solar system integrations is roundoff error (e.g. Quinn & Tremaine 1990). Roundoff errors generally act like spurious dissipation, introducing secular drift in the energy, and hence positional errors  $\propto T^2$ . More precisely, if  $\delta$  is the floating point precision, and  $P$  the orbital period, the expected longitude error after time  $T$  is  $\Delta\lambda \approx T^2\delta/(\tau P)$ . For a 5 Gyr integration with a 1 week timestep, at least 76 bits are needed to keep the roundoff contribute to Mercury's longitude error below 0.01 radians. (Of course, 0.01 radians is much smaller than the expected integration errors, which are inflated by weak chaos, but it is good to set low tolerances for roundoff error, because it is an unphysical effect.) IEEE double precision provides a mantissa of only 53 bits. Many compilers offer quadruple precision, but that is implemented in software, and is slower by a factor of 20 at least.

Our new method offers a significant improvement in effective precision with only a small sacrifice of speed. The reason is that the perturbative impulses ( $u$  and  $v$  in equation [9]) are by far the major computational cost. For a 1 week timestep and  $\epsilon \sim 10^{-3}$ , these impulses are  $10^{-4}$  smaller than  $p, q$ ; hence they require  $\simeq 13$  bits less precision. So by doing the force calculation in double precision and the few remaining operations in quadruple precision, one can effectively gain  $\simeq 13$  bits of precision.

Also, some floating point units (including the Intel  $n86$  series and the Motorola  $68n$  series) use 80 bits internally and compilers for these may offer an extended double precision type with a 64-bit mantissa. On such hardware, we expect that an effective precision of  $\simeq 77$  bits will cost  $< 20\%$  more time than IEEE double precision.

Similar games can be played with other integrators, of course, but generally with less success. In multistep integrators (see Quinlan & Tremaine 1990) force includes the solar part, so the gain in effective precision is less. In generalized leapfrog, there is a large subset of operations not involving small quantities, and when done in quadruple precision these slow the method  $\simeq 6$  fold.

In summary, when roundoff is considered, we estimate that the parallel algorithm running on 1000 processors will be about 50 times faster than generalized leapfrog (as implemented in ST94) on a single processor.

To close this paper, we mention some avenues which may lead to more efficient parallel algorithms.

- 1) Rather than devote 1 processor to each of  $N$  timesteps, it might be better to set  $K$  processors working in parallel on each of  $N/K$  timesteps. Let us assume (i) that using  $K$  processors reduces the time needed to complete a timestep by a factor  $K/g$  where  $g > 1$  represents the degree of parallelism ( $g$  will generally be an increasing function of  $K$ ), and (ii) that the number of iterations required for convergence at timestep  $m$  is  $n(m) = cm + n_0$ , where  $c$  and  $n_0$  are constants (cf. eq. 19). Then parallelizing each timestep is faster if the number of processors  $N > n_0K(g - 1)/[c(K - g)]$ ; for  $K \gg 1$  and the parameters of equation (19) this yields  $N > 6000(g - 1)$ .
- 2) The iterations converge much more quickly near the start of a block of timesteps than near the end. Thus the early processors become free while the later ones are still converging. These freed processors could immediately start working on the next block of timesteps, using the partial converged results from the previous block as a starting point.
- 3) In our implementation, we have not paid much attention to algebraic simplifications, using the chain rule to convert accelerations from cartesian variables to Poincaré elements. It would be worth some effort to try to recast the change of variables, for the chain rule is an arithmetic glutton. An intriguing possibility is that one might be able to dispense with the Poincaré

variables, and simply use the method on the variables  $a, \lambda, e \cos(\Omega + \omega), e \sin(\Omega + \omega), i \cos \Omega, i \sin \Omega$ ; the accelerations would be just the right sides of Gauss's equations for these variables, which are relatively simple to evaluate. Now, the latter variables are not canonical, so the integrator will not be symplectic; but it will still be time-symmetric, and possibly that is good enough. An alternative approach would be to design an iteration scheme based on a generalized leapfrog integrator rather than the implicit midpoint method.

- 4) Our iteration scheme (9) is only linearly convergent. It would be interesting to seek an efficient quadratically convergent iteration scheme.

We thank Wayne Hayes, Matt Holman, Agris Kalnajs, and George Lake for discussions. PS is grateful to the University of Washington for their hospitality. This research was supported by NSERC.

#### APPENDIX: THE IMPLICIT MIDPOINT METHOD

This Appendix derives the error Hamiltonian associated with the implicit midpoint method (3), following Feng (1986).

Let  $\mathbf{z}$  and  $\mathbf{w}$  be vectors of the type  $(p_1, \dots, p_K, q_1, \dots, q_K)$  in phase space. In the following we will use matrix notation:  $\mathbf{z}$  denotes a column vector,  $\mathbf{z}^T$  the corresponding row vector, and so on;  $\mathbf{J}$  is the usual symplectic matrix.

Consider a map that takes  $\mathbf{z}(0)$  to  $\mathbf{z}(t)$ , through a generating function. We write

$$\begin{aligned} \mathbf{z} &= \mathbf{z}(t), & \mathbf{z}_0 &= \mathbf{z}(0), \\ \mathbf{w} &= \frac{1}{2}(\mathbf{z} + \mathbf{z}_0), & \phi &= \phi(\mathbf{w}, t), \end{aligned} \tag{A1}$$

and subscripts for gradients and time derivatives, like  $\phi_{\mathbf{w}}$  and  $\phi_t$ . The map is

$$\mathbf{z} - \mathbf{z}_0 = \mathbf{J}^{-1} \phi_{\mathbf{w}}, \tag{A2}$$

( $\phi_{\mathbf{w}}$  being a gradient). This map is canonical.<sup>1</sup>

Now take the time derivative of (A2), which yields

$$\left(\mathbf{I} - \frac{1}{2}\mathbf{J}^{-1}\phi_{\mathbf{w}\mathbf{w}}\right)\dot{\mathbf{z}} = \mathbf{J}^{-1}\phi_{\mathbf{w}t} \tag{A3}$$

Let us now define a function  $\tilde{H}(\mathbf{z}, t)$  through

$$\phi_t(\mathbf{w}, t) = \tilde{H}(\mathbf{z}, t), \quad \mathbf{z} = \mathbf{w} - \frac{1}{2}\mathbf{J}\phi_{\mathbf{w}}, \tag{A4}$$

---

<sup>1</sup> There are several ways of proving that maps of the type (A2) are canonical, and here is one. If  $\mathbf{x}$  and  $\mathbf{y}$  are two phase space vectors, then the map  $\mathbf{x} \rightarrow \mathbf{y}$  will be canonical if  $\mathbf{x}^T \mathbf{J} d\mathbf{x} - \mathbf{y}^T \mathbf{J} d\mathbf{y}$  is an exact differential. Let  $\mathbf{w} = \frac{1}{2}(\mathbf{x} + \mathbf{y})$ , and suppose that

$$\frac{1}{2}(\mathbf{x}^T \mathbf{J} d\mathbf{x} - \mathbf{y}^T \mathbf{J} d\mathbf{y}) = d\phi + d(\mathbf{w}^T \mathbf{J} \mathbf{x}),$$

for some  $\phi(\mathbf{w}, t)$ . Substituting for  $d\mathbf{y}$ , gives

$$(\mathbf{x} - \mathbf{y})^T \mathbf{J} d\mathbf{w} = d\phi,$$

and hence

$$\mathbf{y} - \mathbf{x} = \mathbf{J}^{-1} \phi_{\mathbf{w}},$$

which is of the form (A2).

the latter relation being a consequence of equation (A2). Taking the gradient of equation (A4) and rearranging gives

$$(\mathbf{I} - \frac{1}{2}\mathbf{J}^{-1}\phi_{\mathbf{w}\mathbf{w}})\mathbf{J}^{-1}\tilde{H}_{\mathbf{z}} = \mathbf{J}^{-1}\phi_{\mathbf{w}t}, \quad (\text{A5})$$

and comparing this with equation (A3) gives

$$\dot{\mathbf{z}} = \mathbf{J}^{-1}\tilde{H}_{\mathbf{z}}(\mathbf{z}, t). \quad (\text{A6})$$

In other words, the map (A2) is equivalent to evolution under the surrogate Hamiltonian  $\tilde{H}$ . Equation (A4) relating the generating function and the surrogate Hamiltonian is a Hamilton-Jacobi equation.

To derive the implicit midpoint method for a system with Hamiltonian  $H$ , we set  $\phi(\mathbf{w}, t) \equiv tH(\mathbf{w})$ ; with this choice equation (A2) evaluated at  $t = \tau$  is identical to equations (3) except for minor differences in notation. The surrogate Hamiltonian for the implicit midpoint method with timestep  $t$  is then defined implicitly by equation (A4), which reads

$$\tilde{H}[\mathbf{w} - \frac{1}{2}t\mathbf{J}H_{\mathbf{w}}(\mathbf{w})] = H(\mathbf{w}). \quad (\text{A7})$$

We may write  $\tilde{H} = H + H_{\text{err}}$ , where the error Hamiltonian may be expanded in a power series,

$$H_{\text{err}} = \sum_{n=1}^{\infty} H_{\text{err}}^n t^n. \quad (\text{A8})$$

By substituting this expansion in (A7) the functions  $H_{\text{err}}^1$ ,  $H_{\text{err}}^2$ , etc. can be determined in succession; for example, assuming  $H$  is autonomous we have

$$H_{\text{err}}^1 = 0, \quad H_{\text{err}}^2 = \frac{1}{8} \sum_{i,j,k,l=1}^{2K} H_i J_{ij} H_{jk} J_{kl} H_l, \quad (\text{A9})$$

where  $H_i = \partial H / \partial w_i$ ,  $H_{ij} = \partial^2 H / \partial w_i \partial w_j$ . Of course, if the system is to be followed over more than one timestep, the factor  $t^n$  in equation (A8) should be replaced by  $[t(\text{mod } \tau)]^n$ .

For a nearly integrable Hamiltonian of the form (5), the error Hamiltonian becomes

$$H_{\text{err}} = \frac{1}{8}\epsilon t^2 \sum_{i,j=1}^K \frac{\partial H^{(0)}}{\partial p_i} \frac{\partial^2 H^{(1)}}{\partial q_i \partial q_j} \frac{\partial H^{(0)}}{\partial p_j} + \mathcal{O}(t^3). \quad (\text{A10})$$

## REFERENCES

- Bellen, A., & Zennaro, M. (1989), *J. Comput. Appl. Math.*, **25**, 341
- Feng, K. (1986), *J. Comp. Math.*, **4**, 279
- Kinoshita, H., Yoshida, H., & Nakai, H. (1991), *Cel. Mech. and Dyn. Astr.*, **50**, 59
- Laskar, J. (1989), *Nature*, **338**, 237
- Laskar, J. (1990), *Icarus*, **88**, 266
- Laskar, J. (1993), *Physica D*, **67**, 257
- Laskar, J. (1994), *Astron. Astrophys.*, **287**, L9
- Laskar, J., & Roboutel, P. (1993), *Nature*, **361**, 608
- Ortega, J.M., & Rheinbolt, W.C. (1970), *Iterative solution of nonlinear equations in several variables*, (Academic Press, New York)
- Quinlan, G. D., & Tremaine, S. (1990), *Astron. J.*, **100**, 1694
- Quinn, T. R., & Tremaine, S. (1990), *Astron. J.*, **99**, 1016
- Quinn, T. R., Tremaine, S., & Duncan, M. (1991), *Astron. J.*, **101**, 2287
- Saha, P., & Tremaine, S. (1992), *Astron. J.*, **104**, 1633
- Saha, P., & Tremaine, S. (1994), *Astron. J.*, **108**, 1962 (ST94)
- Sussman, G. J., & Wisdom, J. (1992), *Science*, **257**, 56
- Touma, J., & Wisdom, J. (1993), *Science*, **259**, 1294
- Wisdom, J., & Holman, M. (1991), *Astron. J.*, **102**, 1528 (WH91)
- Wisdom, J., & Holman, M. (1992), *Astron. J.*, **104**, 2022
- Wisdom, J., Holman, M., & Touma, J. (1994), in *Integration Algorithms for Classical Mechanics*, proceedings of a workshop at the Fields Institute (WHT94)